ELSEVIER

Journal of Organometallic Chemistry 550 (1998) 347–353

Journal of Organometallic Chemistry

9,10-Dimetallatriptycenes of group 14: a structural study [1]

Matheus A. Dam [a], Franciscus J.J. de Kanter [a], Friedrich Bickelhaupt [a,*], Wilberth J.J. Smeets [b], Anthony L. Spek [b], Jorge Fornies-Camer [c], Christine Cardin [c]

[a] *Scheikundig Laboratorium, Vrije Universiteit, De Boelelaan 1083, NL-1081 HV Amsterdam, The Netherlands*

[b] *Bijvoet Center for Biomolecular Research, Vakgroep Kristal- en Structuurchemie, Utrecht University, Padualaan 8, NL-3584 CH Utrecht, The Netherlands*

[c] *Chemistry Department, University of Reading, Whiteknights, Reading RG4 9BB, UK*

Received 20 March 1997

Abstract

From *ortho*-phenylenemagnesium (**1**), 9-phenyl-9-germa-10-silatriptycene (**5**) was prepared via a simple one pot procedure. The previously prepared 9-methyl-10-phenyl-9,10-digermatriptycene (**4**) and **5** are the first germanium-containing 9,10-dimetallatriptycenes to be structurally characterised. The availability of these structural data allows a comparative discussion of 9,10-dimetallatriptycenes of Group 14. © 1998 Elsevier Science B.V.

Keywords: Silicon; Germanium; Tin; 9,10-Dimetallatriptycenes; *ortho*-Phenylenemagnesium

1. Introduction

Recently, we reported a novel synthetic application of the bifunctional organomagnesium compound *ortho*-phenylenemagnesium (**1**) [1], via which 9,10-dimetallatriptycenes of group 14 are readily accessible [2]: reaction of **1** with methyl substituted metal trihalides furnished new 9,10-dimethyl-9,10-dimetallatriptycenes (**3**: $M^1 = M^2 =$ Si, Ge or Sn) (Scheme 1). The reaction could even be tuned to furnish the unsymmetrically substituted 9-methyl-10-phenyl-9,10-digermatriptycene **4** ($R^1 =$ Ph, $R^2 =$ Me, $M^1 = M^2 =$ Ge). This was achieved by the reaction of three equivalents of **1** with one equivalent of trichlorophenylgermane and transformation of the selectively formed tri-Grignard reagent **2** ($R^1 =$ Ph, $M^1 =$ Ge) with one equivalent of trichloromethylgermane to **4**.

In principle, this stepwise one pot approach may give access to a large variety of 9,10-dimetallatriptycenes with different metals and different substituents. This is illustrated by the synthesis of 9-phenyl-9-germa-10-silatriptycene (**5**).

2. Results and discussion

2.1. Synthesis of 9-phenyl-9-germa-10-silatriptycene (5)

Treatment of **1** at −15°C in THF with trichlorophenylgermane, followed by the addition of trichlorosilane, furnished **5** (Scheme 2), which, after elution over silica gel and recrystallisation from toluene was isolated in 76% yield.

2.2. X-ray crystal structures of 9-methyl-10-phenyl-9,10-digermatriptycene (4) and 10-phenyl-10-germa-9-silatriptycene (5)

Single crystals of **5** suitable for X-ray crystal structure determination were obtained upon slow diffusion of *n*-hexane from the gas phase into a toluene solution of **5**. Similarly, we were able to obtain the crystal structure of **4**; the availability of three structures of 9,10-dimetallatriptycenes of Group 14, that is, that of **4**, **5**, and the previously determined structure of **3c** [2], together with the reported structure of 9-hydroxy-10-methyl-9,10-disilatriptycene **6** ($M^1 = M^2 =$ Si, $R^1 =$ Me, $R^2 =$ OH) [3],

* Corresponding author. Tel.: +31 20 4447479. Fax: +31 20 4447488. E-mail: bickelhpt@chem.vu.nl.

[1] Dedicated to Prof. Dr. K. Wade at the occasion of his 65th birthday in friendship and appreciation.

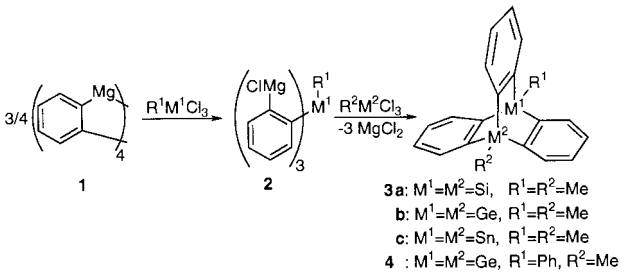

Scheme 1. Synthesis of substituted 9,10-dimetallatriptycenes **3** and **4**.

allows a comparative discussion of this novel class of compounds.

The solid state structures of **4** and **5** are depicted in Figs. 1 and 2, respectively. Crystal data, data collection, and refinement parameters are reported in Table 1. Fractional atomic coordinates and equivalent thermal parameters of **4** and **5** are presented in Tables 2 and 3, respectively. Selected bond distances and bond angles of **4** and **5**, together with the corresponding values for **3c** and **6**, are listed in Table 4.

Fig. 1 shows that in **4**, the phenyl substituent is disordered over two orientations with respect to the triptycene skeleton; the two orientations are represented by C(8)-C(13) and C(81)-C(131). These orientations are populated in a 1:1 ratio and they probably result from packing effects. Pairs of molecules of **4** pack together, each with its own disordered phenyl group orientation to avoid collision. In the ^{1}H and ^{13}C NMR spectra of both **4** and **5** (Tol-d_8: 298–198 K), only one set of signals is observed for the phenyl substituent, indicating that in solution there is no hindered rotation around the Ge–C(phenyl) axis.

It appears (Table 4) that **4** and **5** are strained and have some general structural features in common. In both **4** and **5** the average 'internal' angles β_n (β_n = M(n)-C_{ipso}-C_{ipso}; see Fig. 3) (**4**: $\beta_1 = 116.1(5)°$, $\beta_2 = 115.0(5)°$, **5**: $\beta_1 = 116.1(5)°$, $\beta_2 = 114.3(5)°$) are smaller and the average 'external angles' γ_n (γ_n = M(n)-C_{ipso}-C: Fig. 3) (**4**: $\gamma_1 = 124.8(5)°$, $\gamma_2 = 125.6(5)°$, **5**: $\gamma_1 = 125.7(7)°$, $\gamma_2 = 125.7(7)°$) are wider than the standard angle of 120°. The average angles α_n (α_n = C_{ipso}-M(n)-C_{ipso}) (**4**: $\alpha_1 = 102.5(4)°$, $\alpha_2 = 102.9(3)°$, **5**: $\alpha_1 = 104.6(5)°$, $\alpha_2 = 101.8(4)°$) are more acute than 109.5°, the ideal angle for sp^3 hybridised bridgehead atoms. These structural deformations indicate that the

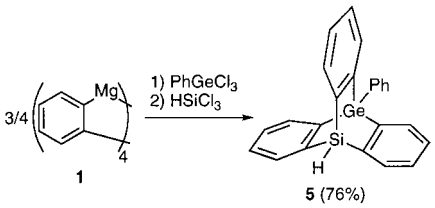

Scheme 2. Synthesis of 10-phenyl-10-germa-9-silatriptycene **5**.

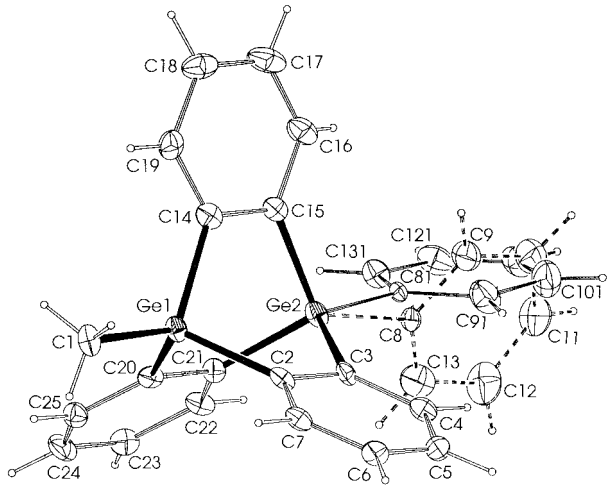

Fig. 1. ORTEP plot of **4** with ellipsoids drawn at 30% probability level.

triptycene skeleton imposes substantial ring strain because, for purely geometric reasons, this arrangement does not simultaneously allow perfectly tetrahedral angles around the bridgehead atoms ($\alpha = 109.4°$) and perfectly trigonal angles around the *ipso*-carbon atoms ($\beta = \gamma = 120°$). For example, when α is artificially fixed at 109.4°, the triptycene skeleton can only be formed with $\beta = 109.5°$ and $\gamma = 130.5°$. Similarly, when β and γ are kept at 120°, α necessarily has to decrease to 97.2°. Not surprisingly, the 'real' molecules choose a compromise between the two extremes.

The geometric restrictions imposed on the bond angles lead to a change in the rehybridisation of the orbitals concerned and this, in turn, has consequences for the bond lengths: in comparison to ideal sp^3 hybridisation, the metal uses more p character in the bridgehead–phenylene bonds in order to make α smaller than 109.4°, and thus more s character is left for the bridge-

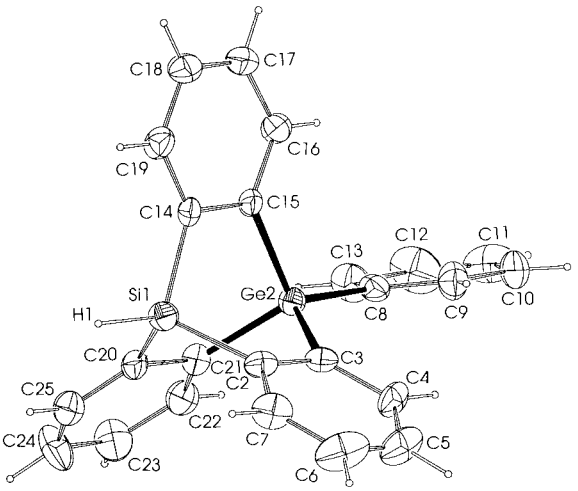

Fig. 2. ORTEP plot of **5** with ellipsoids drawn at 30% probability level.

Table 1
Crystal data, data collection, and refinement parameters for the 9,10-dimetallatriptycenes **4** and **5**

	4	**5**
Crystal data		
Formula	$C_{25}H_{20}Ge_2$	$C_{24}H_{18}GeSi$
Molecular weight	465.65	407.06
Crystal system	monoclinic	orthorhombic
Space group	$P2_1/c$ (No. 14)	$P2_12_12_1$ (No. 19)
a (Å)	11.889(4)	10.679(5)
b (Å)	10.054(5)	12.082(5)
c (Å)	17.417(9)	14.942(6)
β (°)	99.36(4)	90
V (Å^3)	2054(2)	1927.9
Z	4	4
D_{calc} (g cm^{-3})	1.506(1)	1.402
F(000)	936	832
μ (cm^{-1})	29.3	16.6
Crystal size (mm)	0.20 × 0.25 × 0.30	0.30 × 0.20 × 0.20
Data collection and refinement		
Temp. (K)	150	293
θ_{min}, θ_{max}	1.19, 25.00	3.37, 25.91
Radiation	MoK α	MoK α
Monochromator	graphite	graphite
λ (Å)	0.71073	0.71073
$\Delta\omega$ (°)	0.99 + 0.35 tanθ	–
Hor. and vert. aperture (mm)	3.00 + 1.50 tanθ, 4.00	–
Reference reflections	2-1-7, 2-2-1, 5-2-2	–
Data set	h −10:14; k −11:0; l −20:20	h 0:13; k 0:14; l 0:17
Total data	4459	13338
Total unique data	3612	2034
No. refined parameters	312	258
Weighting scheme[a]	a = 0.0646, b = 4.48	a = 0.0590, b = 1.35
Final R1[b]	0.0590	0.0407
wR2[c]	0.1429	0.1175
S[d]	1.042	1.156
$(\Delta/\sigma)_{av}$ and $(\Delta/\sigma)_{max}$ in final cycle	0.000, 0.001	–

[a] Weighting scheme = $1/[\sigma^2(Fo^2) + (a*P)^2 + b*P]$.
[b] $R1 = [\Sigma(||Fo| - |Fc||)/\Sigma|Fo|]$.
[c] $wR2 = [\Sigma[w(Fo^2 - Fc^2)^2]/\Sigma[w(Fo^2)^2]]^{0.5}$.
[d] $S = [\Sigma[w(Fo^2 - Fc^2)^2]/(n - p)]^{0.5}$.

head–substituent bonds. Consequently the bridgehead–substituent bonds of the 9,10-dimetallatriptycenes **4** and **5** will be shortened while the bridgehead–phenylene bonds will be stretched in comparison to those of unstrained model compounds, as has been observed for all-carbon triptycenes [9]. For example, the bridgehead–substituent bonds in **4** and **5** (**4**: Ge(1)-C(1) = 1.938(7) Å, Ge(2)-C(8/81) = 1.94(2) Å; **5**: Si(1)-H(1) = 1.468(39) Å, Ge(2)-C(8) = 1.944(4) Å) are relatively short when compared to those in unstrained compounds with analogous substitution patterns (Ge-C(methyl) = 1.951(8) Å [4]; Si-H = 1.491(28) Å [5]; Ge-C(aryl) = 1.954(1) [6], 1.948(4) Å [7]). On the other hand, the average bridgehead–phenylene bonds (**4**: Ge(1)-C_{ipso} = 1.952(7) Å, Ge(2)-C_{ipso} = 1.956(7) Å; **5**: Si(1)-C_{ipso} = 1.869(8) Å, Ge(2)-C_{ipso} = 1.961(6) Å) are slightly longer than those in unstrained model compounds (Ge-C_{ipso} = 1.954(5) Å [4], 1.954(1) [6], 1.948(4) Å [7]; Si-C_{ipso} = 1.85(1) Å [5], 1.852(13) Å [8]). In the case of **4**, the differences are within the range of the experimental error, but the trend observed is consistent. In this context it has to be noted that the observed elongation of the bridgehead–phenylene bonds is expected to be less pronounced than the shortening of the bridgehead–substituent bonds because, per bridgehead atom, the total amount of reduced s character is spread over three bridgehead–phenylene bonds while the identical amount of enhanced s character appears in only one bridgehead–substituent bond.

Generally speaking, the 9,10-disilatriptycene **6** [3] and the 9,10-distannatriptycene **3c** [2] show similar trends to **4**. For example, all three compounds have relatively short M–R bonds and relatively long M–C_{ipso} bonds, the angles α and β are more acute than 109.4°

Table 2
Fractional atomic coordinates and equivalent thermal parameters of **4** with estimated standard deviations in parentheses

Atom	x	y	z	U_{eq}^{a} (Å^2)
Ge(1)	0.56816(6)	0.60153(7)	0.20726(4)	0.0234(2)
Ge(2)	0.79098(6)	0.48361(7)	0.16540(5)	0.0254(3)
C(1)	0.4275(6)	0.6750(7)	0.2317(5)	0.034(3)
C(2)	0.5494(6)	0.4641(7)	0.1281(4)	0.025(2)
C(3)	0.6498(6)	0.4103(6)	0.1075(4)	0.024(2)
C(4)	0.6437(6)	0.3138(7)	0.0499(4)	0.029(2)
C(5)	0.5380(7)	0.2668(7)	0.0140(4)	0.032(2)
C(6)	0.4393(6)	0.3183(7)	0.0339(4)	0.029(2)
C(7)	0.4451(6)	0.4155(7)	0.0901(4)	0.027(2)
* C(8)	0.927(2)	0.409(3)	0.1245(11)	0.023(4)
* C(9)	0.9751(18)	0.299(2)	0.1604(12)	0.049(5)
* C(10)	1.070(3)	0.247(4)	0.1353(17)	0.056(7)
* C(11)	1.1164(17)	0.308(2)	0.0797(13)	0.055(5)
* C(12)	1.0582(17)	0.408(2)	0.0392(12)	0.063(5)
* C(13)	0.9605(18)	0.461(2)	0.0671(11)	0.061(5)
C(14)	0.6704(6)	0.5171(7)	0.2930(4)	0.028(2)
C(15)	0.7698(6)	0.4593(7)	0.2735(4)	0.025(2)
C(16)	0.8462(6)	0.3963(7)	0.3313(5)	0.037(3)
C(17)	0.8259(8)	0.3894(9)	0.4065(5)	0.047(3)
C(18)	0.7318(7)	0.4507(8)	0.4265(5)	0.041(3)
C(19)	0.6530(7)	0.5143(7)	0.3695(4)	0.033(3)
C(20)	0.6713(6)	0.7299(7)	0.1707(4)	0.025(2)
C(21)	0.7731(5)	0.6767(7)	0.1516(4)	0.023(2)
C(22)	0.8497(6)	0.7619(7)	0.1249(4)	0.028(2)
C(23)	0.8282(6)	0.8976(8)	0.1176(4)	0.031(2)
C(24)	0.7289(7)	0.9481(8)	0.1369(4)	0.037(3)
C(25)	0.6502(6)	0.8641(7)	0.1637(4)	0.028(2)
* C(81)	0.9329(18)	0.411(2)	0.1526(12)	0.018(5)
* C(91)	0.9443(17)	0.285(2)	0.1188(13)	0.048(6)
* C(101)	1.048(3)	0.229(3)	0.1109(17)	0.053(7)
* C(111)	1.1477(17)	0.311(2)	0.1327(12)	0.047(6)
* C(121)	1.1420(14)	0.4343(18)	0.1617(10)	0.045(5)
* C(131)	1.0362(12)	0.4837(15)	0.1732(9)	0.032(4)

[a] U_{eq} is defined as one third of the trace of the orthogonalized U_{ij} tensor.
* Indicates site occupation factor = 0.50.

Table 3
Fractional atomic coordinates and equivalent thermal parameters of **5** with estimated standard deviations in parentheses

Atom	x	y	z	U_{eq}^{a} (Å^2)
Si(1)	0.7504(3)	0.3401(1)	0.0523(1)	0.044(1)
Ge(2)	0.7502(1)	0.5609(1)	0.1507(1)	0.038(1)
H(1)	0.7418(64)	0.2323(33)	0.0047(28)	0.035(11)
C(2)	0.8859(7)	0.4332(10)	0.0265(6)	0.046(2)
C(3)	0.8928(8)	0.5327(8)	0.0682(6)	0.042(2)
C(4)	0.9857(6)	0.6087(10)	0.0473(9)	0.056(3)
C(5)	1.0710(8)	0.5843(13)	−0.0191(9)	0.075(4)
C(6)	1.0666(12)	0.4850(10)	−0.0623(10)	0.087(5)
C(7)	0.9778(7)	0.4074(11)	−0.0404(8)	0.062(3)
C(8)	0.7512(12)	0.6990(3)	0.2175(3)	0.045(1)
C(9)	0.8586(9)	0.7470(10)	0.2448(7)	0.069(3)
C(10)	0.8707(14)	0.8423(11)	0.2938(7)	0.092(4)
C(11)	0.7531(22)	0.8922(5)	0.3189(5)	0.110(3)
C(12)	0.6496(15)	0.8474(13)	0.2926(8)	0.104(5)
C(13)	0.6358(9)	0.7484(9)	0.2416(7)	0.070(3)
C(14)	0.7489(11)	0.3254(3)	0.1760(3)	0.041(1)
C(15)	0.7512(11)	0.4274(3)	0.2244(3)	0.040(1)
C(16)	0.7524(11)	0.4268(4)	0.3174(3)	0.049(1)
C(17)	0.7503(11)	0.3273(4)	0.3638(3)	0.058(1)
C(18)	0.7521(14)	0.2288(4)	0.3185(4)	0.057(1)
C(19)	0.7515(13)	0.2284(4)	0.2264(3)	0.051(1)
C(20)	0.6126(7)	0.4301(9)	0.0237(7)	0.045(2)
C(21)	0.6107(7)	0.5375(9)	0.0696(6)	0.043(2)
C(22)	0.5175(8)	0.6108(9)	0.0483(8)	0.058(3)
C(23)	0.4266(11)	0.5847(11)	−0.0134(9)	0.078(4)
C(24)	0.4305(13)	0.4843(10)	−0.0593(9)	0.086(5)
C(25)	0.5243(8)	0.4080(10)	−0.0381(8)	0.062(3)

U_{eq} is defined as one third of the trace of the orthogonalized U_{ij} tensor.

and 120°, respectively, and the angles γ are larger than 120°. However, careful examination of the angles α, β and γ of **6**, **4** and **3c** reveals some influence of the bridgehead atom: deviations of β and γ from 120°

Table 4
Selected bond distances (Å) and bond angles (°) of 9,10-dimetallatriptycenes **3c**, **4**, **5** and **6** with estimated standard deviations in parentheses (see Fig. 3)

	6[a] M(1) = Si, R(1) = Me M(2) = Si, R(2) = OH	**5**[b] M(1) = Si, R(1) = H M(2) = Ge, R(2) = Ph	**4**[b] M(1) = Ge, R(1) = Me M(2) = Ge, R(2) = Ph	**3c**[c] M(1) = Sn, R(1) = Me M(2) = Sn, R(2) = Me
M(1)-R(1)	1.835	1.468(39)	1.938(7)	2.113(4)
M(2)-R(2)	1.636	1.944(4)	1.94(2)[d]	2.113(4)
M(1)-C_{ipso}^{d}	1.870	1.869(8)	1.952(7)	2.153(2)
M(2)-C_{ipso}^{d}	1.864	1.961(6)	1.956(7)	2.153(2)
C_{ipso}-C_{ipso}^{d}	1.416	1.42(2)	1.41(1)	1.405(3)
α_1 (C_{ipso}-M(1)-C_{ipso})[d]	103.01	104.6(4)	102.5(4)	101.42(9)
α_2(C_{ipso}-M(1)-C_{ipso})[d]	104.23	101.8(4)	102.9(3)	101.42(9)
β_1(M(1)-C_{ipso}-C_{ipso})[d]	115.70	116.1(5)	116.1(5)	117.4(2)
β_2(M(2)-C_{ipso})-C_{ipso})[d]	113.94	114.3(5)	115.0(5)	117.4(2)
γ_1(M(1)-C_{ipso}-C)[d]	126.08	125.7(7)	124.8(5)	124.1(2)
γ_2(M(1)-C_{ipso}-C)[d]	126.27	125.7(7)	125.6(5)	124.1(2)

[a] From [3].
[b] This work.
[c] From [2].
[d] Average value.

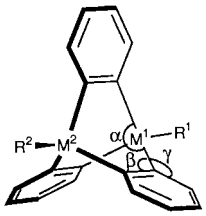

Fig. 3. Characteristic angles in the triptycene skeleton.

decrease from silicon (**6**) via germanium (**4**) to tin (**3c**), while deviations of α from 109.4° increase in the same direction. These observations can be explained by the difference in hardness between silicon, germanium and tin. In the case of silicon, which is relatively hard, deviations from the tetrahedral environment around the metal atom are more difficult (large α); this goes at the expense of a larger deviation in the angles β and γ in order to allow the closure of the triptycene skeleton. Germanium is softer and allows a larger deformation of its tetrahedral environment (small α). Consequently, to meet the geometrical requirements, smaller deviations of the angles β and γ at the benzene rings are feasible. For tin, which is softer than germanium, these trends are even more pronounced.

3. Conclusions

The synthesis of 9-phenyl-9-germa-10-silatriptycene (**5**) demonstrates that our synthetic approach towards 9,10-dimetallatriptycenes is quite versatile. The availability of the crystal structures of **5** and **4** allowed a comparative study of 9,10-dimetallatriptycenes of Group 14, which furnished a consistent interpretation of the specific bonding situation at the bridgehead position of these species.

4. Experimental

Reactions were performed in fully sealed glassware using standard high vacuum techniques. **1** and **4** were prepared according to literature [1,2]. Metal trihalides were commercially purchased. Solvents were dried by distillation from liquid Na/K alloy after pre-drying on NaOH. NMR spectra were measured at 25°C on a Bruker MSL 400 spectrometer (^{1}H NMR: 400.1 MHz: ^{13}C NMR: 100.6 MHz). ^{13}C, ^{1}H COSY and ^{1}H NOE experiments were used for spectral assignment. HRMS measurements were performed on a Finnigan MAT 90 mass spectrometer (direct inlet). Melting points are uncorrected. Elemental analysis was carried out at the Mikroanalytisches Labor Pascher, Remagen, Germany.

4.1. 9-Phenyl-9-germa-10-sila-triptycene (5)

(Fig. 4)

At −15°C, a solution of trichlorophenylgermane (0.350 g; 1.37 mmol) in 7.37 ml of toluene was added during 20 min to a solution of **1** (4. 10 mmol of the formal monomeric unit C_6H_4Mg) in 100.0 ml of THF. After additional stirring at −15°C for 2 h, trichlorosilane (0.186 g; 1.37 mmol) in 20.0 ml of benzene was added during 45 min. The reaction mixture was stirred for 2 h at −15°C and 1 h at 5°C, after which it was allowed to warm to room temperature overnight. The mixture was quenched with saturated ammonium chloride solution and extracted with toluene (3 × 20 ml). The combined organic layers were dried ($MgSO_4$), filtered and the solvent was evaporated in vacuo. The residue was dissolved in benzene and eluted from silica. Evaporation (in vacuo) of the solvent furnished the crude product, which was recrystallised from toluene (2 ×) to yield **5** as colourless crystals. Yield: 0.423 g (76%); mp: > 260°C.

^{1}H NMR (400 MHz, $CDCl_3$): δ = 7.96 (m, ^3J(H,H) = 7.5 Hz, ^4J(H,H) = 1.4 Hz, ^4J(H,H) = 1.3 Hz, ^5J(H,H) = 0.7 Hz, 2H; H(18)), 7.79 (dq, ^3J(H,H) = 7.2 Hz, ^4J(H,H) = 1.3 Hz, ^5J(H,H) = 0.8 Hz, 3H; H(4,5,16)), 7.72 (bm, ^3J(H,H) = 7.3 Hz, ^4J(H,H) = 1.2 Hz, ^5J(H,H) = 0.8 Hz, ^5J(H,H) = 0.5 Hz, 3H; H(1,8,13)), 7.33 (m, ^3J(H,H) = 7.5 Hz, ^4J(H,H) = 1.4 Hz, 1H; H(20)), 7.32 (m, ^3J(H,H) = 7.6 Hz, ^3J(H,H) = 7.5 Hz, ^4J(H,H) = 1.3 Hz, ^5J(H,H) = 0.7 Hz, 2H; H(19)), 7.06 (m, ^3J(H,H) = 7.6 Hz, ^3J(H,H) = 7.2 Hz, ^4J(H,H) = 1.2 Hz, 3H; H(3,6,15)), 7.02 (m, ^3J(H,H) = 7.6 Hz, ^3J(H,H) = 7.3 Hz, ^4J(H,H) = 1.3 Hz, 3H; H(2,7,14)), 5.67 (bs, ^1J(Si,H) = 214.7 Hz, 1H; H(10)); ^{13}C NMR (100 MHz, C_6D_6): δ = 148.2 (m; C(8a,9a,12)), 142.1 (dq, ^1J(C,Si) = 67.0 Hz, ^3J(C,H) = 6.9 Hz, ^2J(C,H) = 4.4 Hz; C(4a,10a,11)), 136.5 (dm, ^1J(C,H) = 160.9 Hz; C(18)), 134.3 (dd, ^1J(C,H) = 165.6 Hz, ^3J(C,H) = 7.0 Hz; C(4,5,16)), 132.3 (dd, ^1J(C,H) = 165.3 Hz, ^3J(C,H) = 6.1 Hz; C(1,8,13)), 130.3 (dt, ^1J(C,H) = 160.1 Hz, ^3J(C,H) = 7.6 Hz; C(20)), 129.3 (dd, ^1J(C,H) = 168.1 Hz, ^2J(C,H) = 5.4 Hz; C(19)), 128.5 (t, ^2J(C,H) = 3.5 Hz; C(17)), 128.0 (dd, ^1J(C,H) = 158.8 Hz, ^3J(C,H) = 5.2 Hz; C(2,7,14)), 127.6 (dd,

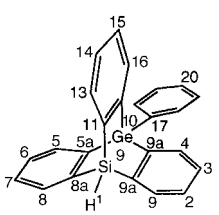

Fig. 4. Numbering of 10-phenyl-10-germa-9-silatriptycene **5** (= 10-phenyl-9,10-dihydro-10-germa-9-sila-9,10[1′,2′]-benzenoanthracene according to IUPAC [10]).

^1J(C,H) = 158.2 Hz, ^3J(C,H) = 6.8 Hz; C(3,6,15)); HRMS: m/z = 404.0420 (Calc. for $C_{24}H_{18}^{28}Si^{70}Ge$ (M^+): m/z = 404.0421). Anal. Calc. for $C_{24}H_{18}GeSi$ (407.1): C, 70.81; H, 4.46. Found: C, 70.55; H, 4.41.

4.2. X-ray structure determinations

4.2.1. X-ray crystallographic analysis of **4**

A colourless block-shaped crystal was mounted on top of a glass fibre (using the inert oil technique) and transferred to the cold nitrogen stream of an Enraf-Nonius CAD4T diffractometer for data collection at 150 K (Rotating anode, 60 kV, 100 mA, graphite-monochromated MoKα radiation, ω-scan mode). Unit cell parameters were determined from a least-squares treatment of the SET4 setting angles of 25 reflections with $10.00 < \theta < 13.77°$. The unit cell parameters were checked for the presence of higher lattice symmetry [11]. A total of 4459 reflections were collected and merged into a data set of 3612 unique reflections. The crystals showed broad reflection profiles and reflected rather poorly. Three intensity control reflections, monitored every hour, showed a decay of 2.6% during the 16.8 h of X-ray exposure time. The structure was solved with direct methods (SHELXS86 [12]) and subsequent difference Fourier analyses. The C(8)–C(13) phenyl ring is disordered over two orientations in a 1:1 ratio. Refinement on F^2 with all unique reflections was carried out by full matrix least-squares techniques. Hydrogen atoms were introduced on calculated positions and included in the refinement riding on their carrier atoms. All non-H atoms were refined with anisotropic thermal parameters; H atoms with isotropic thermal parameters related to the U_{eq} of the carrier atoms.

Weights were introduced in the final refinement cycles, convergence was reached at R1 = 0.0590 (for 2487 reflections with $Fo > 4\sigma(Fo)$), wR2 = 0.1429 (for all unique reflections). A final difference Fourier map shows no features outside the range $-0.80:+0.88$ e/Å^3.

Crystal data and numerical details of the structure determination are given in Table 1. Final atomic coordinates and equivalent isotropic thermal parameters are listed in Table 2.

Neutral atom scattering factors and anomalous dispersion factors were taken from [13]. All calculations were performed with SHELXL96 [14] and the PLATON [15] package (geometrical calculations and illustrations) on a DEC-5000 cluster. Full details may be obtained from one of the authors (A.L.S.).

4.2.2. X-ray crystallographic analysis of **5**

Suitable crystals of **5** were grown by slow diffusion of *n*-hexane from the gas phase into a solution of the compound in toluene and mounted on a glass fibre. The data collection and processing was performed at room temperature on a Mar Research image plate scanner, graphite-monochromated Mo–Kα radiation used to measure 95 2° frames, 180 sec. per frame.

XDS package [16] was used to give 2034 unique reflections (merging R = 0.0250). The heavy atoms were found from the Patterson map using the SHELX90 [17] program and refined subsequently from successive difference Fourier maps using SHELXL [18], by full-matrix least-squares of 258 variables, to a final R factor of 0.0407 for 2025 reflections with $[Fo] > 4\sigma(Fo)$. All atoms were revealed by the Fourier map difference including H(1). Non hydrogen atoms were refined anisotropically. Aromatic hydrogen atoms were placed geometrically and then refined with fixed isotropic atomic displacement parameter. The weighting scheme $w = 1/[\sigma^2(Fo^2) + (a \times P)^2 + (b \times P)$ where $P = (Max(Fo^2, 0) + 2Fc^2)/3$, a = 0.0590 and b = 1.35 with $\sigma(Fo)$ from counting statistics gave satisfactory agreement analyses. Data collection parameters including R1 ($[Fo] > 4\sigma(Fo)$) and wR2 (all data) values are summarized in Table 1. Full details may be obtained from one of the authors (C.C.).

Acknowledgements

This work was supported in part (M.A.D., W.J.J.S. and A.L.S.) by the Netherlands Foundation for Chemical Research (SON) with financial aid from the Netherlands Organisation for Scientific Research (NWO), which is gratefully acknowledged. The cooperation between the groups in Amsterdam and Reading was stimulated by the Human Capital and Mobility Programme of the European Union (Contract No. ERBCHRXCT930281).

References

[1] M.A.G.M. Tinga, G. Schat, O.S. Akkerman, F. Bickelhaupt, E. Horn, H. Kooijman, W.J.J. Smeets, A.L. Spek, J. Am. Chem. Soc. 115 (1993) 2808.
[2] M.A. Dam, O.S. Akkerman, F.J.J. De Kanter, F. Bickelhaupt, N. Veldman, A.L. Spek, Chem. Eur. J. 2 (1996) 1139.
[3] M. Takahashi, K. Hatano, Y. Kawada, G. Koga, N. Tokitoh, R. Okazaki, J. Chem. Soc. Chem. Comm. (1993) 1850.
[4] O.A. D'yachenko, S.V. Soboleva, L.O. Atovmyan, J. Struc. Chem. USSR 17 (1976) 426 (Zh. Struk. Khim. 17 (1976) 496).
[5] O.A. D'yachenko, L.O. Atovmyan, S.V. Soboleva, T.Yu. Markova, N.G. Komalenkova, L.N. Shamshin, E.A. Chernyshev, J. Struc. Chem. USSR 15 (1974) 161 (Zh. Struk. Khim. 15 (1974) 170); O.A. D'yachenko, L.O. Atovmyan, S.V. Soboleva, J. Struc. Chem. USSR 16 (1975) 478 (Zh. Struk. Khim. 16 (1975) 505).
[6] P.C. Chieh, J. Chem. Soc. (A), (1971) 3241.
[7] M. Charissé, S. Roller, M. Dräger, J. Organometal. Chem. 427 (1992) 23.
[8] J. Allemand, R. Gerdil, Cryst. Struct. Comm. 8 (1979) 927.
[9] M. Ôki, M. Matsusue, T. Akinaga, Y. Matsumoto, S. Toyota, Bull. Chem. Soc. Jpn. 67 (1994) 2831; M. Ôki, N. Takiguchi, S.

Toyota, G. Yamamoto, S. Murata, Bull. Chem. Soc. Jpn. 61 (1988) 4295; F. Imashiro, K. Hirayama, K. Takegoshi, T. Terao, A. Saika, Z. Taira, J. Chem. Soc. Perkin Trans. II (1988) 1401; M. Ôki, G. Izumi, G. Yamamoto, N. Nakamura, Bull. Chem. Soc. Jpn. 55 (1982) 159; M. Mikami, K. Toriumi, M. Konno, Y. Saito, Acta Crystallogr. B31 (1975) 2474; N. Nogami, M. Ôki, S. Sato, Y. Saito, Bull. Chem. Soc. Jpn. 5 (1982) 3580.

[10] J. Rigaudy, S.P. Klesney, IUPAC Nomenclature of Organic Chemistry, Pergamon, Oxford, 1979, p. 35.

[11] A.L. Spek, J. Appl. Crystallogr. 21 (1988) 578.

[12] G.M. Sheldrick, SHELXS86. Program for Crystal Structure Determination, Univ. Göttingen, 1986.

[13] A.J.C. Wilson (Ed.), International Tables for Crystallography, Volume C. KIuwer, Dordrecht, The Netherlands, 1992.

[14] G.M. Sheldrick, SHELXL96. Program for Crystal Structure Determination, Univ. Göttingen, 1996.

[15] A.L. Spek, Acta Crystallogr. A46 (1990) C34.

[16] W. Kabsch, J. Appl. Crystallogr. 26 (1993) 795.

[17] G.M. Sheldrick, Acta Crystallogr. A46 (1990) 467.

[18] G.M. Sheldrick, J. Appl. Crystallogr. (1997), in prep.